Clay Minerals (2021), **56**, 250–259
doi:10.1180/clm.2022.3

CAMBRIDGE UNIVERSITY PRESS

Article

Esterification of naphthenic acids with various structures over tungstophosphoric acid-intercalated layer double hydroxide catalysts with various interlayer spacings

Yan Wu[1], Shiang He[1], Dongmei Li[1], Yang Li[2] and Hao Wang[1]*

[1]School of Chemistry and Chemical Engineering, Southwest Petroleum University, Chengdu 610500, China and [2]Petrochemical Research Institute, PetroChina Co. Ltd, Beijing 102206, China

Abstract

Tungstophosphoric acid-intercalated MgAl layer double hydroxides (LDHs) are active catalysts for removing naphthenic acids (NAs) from petroleum *via* esterification. Due to their active sites being in the interlayer, the interlayer spacing of LDHs might affect their activity, particularly for NAs with various structures. Herein, two tungstophosphoric acid-intercalated MgAl LDHs with various interlayer spacings (d_{003} = 1.46 and 1.07 nm) synthesized by varying the ion-exchange time were used as catalysts for esterification between NAs and ethylene glycol. Six NAs with various side chains and rings were used as model compounds to investigate the effects of NA structures and d_{003} values on the activity of LDHs. In general, NAs with large molecule sizes and steric hindrances are less reactive over the same catalyst. The LDH with a larger d_{003} value favours the esterification of NAs regardless of their structure, particularly NAs with large molecule sizes and steric hindrances. However, a large d_{003} is less effective for esterification of NAs with conjugated carboxyl groups. An enlarged interlayer space might facilitate NA molecules to access the interlayer of LDHs so as to come into contact with the catalytic sites, making this process responsible for the enhanced reactivity. The esterification kinetics of cyclohexanecarboxylic acid over these LDHs follow a first-order reaction. The activation energies for the LDHs with large and small d_{003} values are 26.25 and 32.18 kJ mol^{-1}, respectively.

Keywords: esterification catalysts, interlayer spacing, kinetics, structure of naphthenic acids, tungstophosphoric acid-intercalated LDHs

(Received 22 July 2021; revised 26 December 2021; Accepted Manuscript online: 10 January 2022; Associate Editor: Chun-Hui Zhou)

Naphthenic acids (NAs) account for >85% of acids in crude oil and are responsible for the acidity of crude oil, resulting in the corrosion to refinery pipes and equipment. In general, crude oils with a total acid number (TAN) >0.5 mg KOH g^{-1} are regarded as acidic oils and pose a corrosion risk for refineries (Wang *et al.*, 2014b). Removing NAs from crude oil is achieved by extraction, adsorption and hydrotreatment, among other processes. However, solvent extraction requires several washing steps that consume large amounts of solvent and cause serious emulsion effects (Redondo *et al.*, 2020). Adsorption requires a large investment in infrastructure, including adsorption, desorption and solvent recovery units; moreover, other highly polar compounds in petroleum reduce the adsorption efficiency (Wang *et al.*, 2014b). Hydrotreatment operations require conditions that are expensive to maintain, such as hydrogen pressures >4 MPa and temperatures >300°C (Wang *et al.*, 2014b). Among the various deacidification methods, esterification between NAs and alcohol is an effective and low-cost approach due to its mild reaction conditions, high yield and few negative effects on the quality of the crude oil (Wang *et al.*, 2014b; Khan *et al.*, 2017).

*E-mail: cprswpu01@163.com

Cite this article: Wu Y, He S, Li D, Li Y, Wang H (2021). Esterification of naphthenic acids with various structures over tungstophosphoric acid-intercalated layer double hydroxide catalysts with various interlayer spacings. *Clay Minerals* **56**, 250–259. https://doi.org/10.1180/clm.2022.3

Heteropolyacids (HPAs) are polyoxometalates composed of heteropolyanions having metal–oxygen octahedra as their basic structural unit. Keggin-type HPAs are the most important in catalysis (Lopez-Salinas *et al.*, 2000). 12-Tungstophosphoric acid ($H_3PW_{12}O_{40}$; HPW) is a stable and strongly acidic HPA with a Keggin structure that can be used as a superior esterification catalyst (Cardoso *et al.*, 2008; Patel & Brahmkhatri, 2013). The disadvantages of HPW are its low surface area and stability (Das & Parida, 2007). The deposition of HPW onto various porous supports can disperse the active sites over a large specific surface area and thus improve the catalytic activity of HPW.

Layered double hydroxides (LDHs) are anionic lamellar minerals represented by the general formula $[M^{2+}_{1-x}M^{3+}_{x}(OH)_2][A^{n-}_{x/n}]\cdot mH_2O$, where M^{2+} and M^{3+} are bi- and tri-valent metal cations, x is the ratio of $M^{3+}/(M^{2+}+M^{3+})$ and A is an interlayer anion (Mao *et al.*, 2017). The LDHs are ideal inorganic supports for immobilizing HPW because their interlayer spaces are very flexible at accommodating guest molecules of various sizes (Ma *et al.*, 2017) and their unique structures can disperse the intercalant effectively (Wang *et al.*, 2017). Introducing HPW anions into the interlayer of LDHs might not only increase the acidity of LDHs, but also improve the stability and dispersion of HPW (Ma *et al.*, 2017; Enferadi-Kerenkan *et al.*, 2018). Thus, HPW-intercalated LDHs can be used as active esterification catalysts (Das & Parida, 2007; Omwoma *et al.*, 2014).

Wu *et al.* (2017b) synthesized HPW-intercalated MgAl, ZnAl and NiAl LDHs as catalysts for removing NAs from crude oil *via* esterification between NAs and ethylene glycol (EG). The introduction of HPW into LDHs improved the esterification activity of LDHs due to their increased acidity. Moreover, the interlayer of LDHs acted as a reactor because the catalytic sites are located in the interlayer. Reactants must be close to the edges of LDHs or enter the interlayer to adsorb and react with the active sites (Hu *et al.*, 1998; Guo *et al.*, 2001). Such a reaction can be considered as an interlayer catalytic reaction in which the interlayer of LDHs provides both the catalytic sites and the reaction field (Wang *et al.*, 2015; She *et al.*, 2021). Some researchers also immobilized the catalytic sites in the interlayer of LDHs and developed various interlayer reactions in a nanosized confined region (An *et al.*, 2006; Shi *et al.*, 2010; Shi & He, 2011; Liu *et al.*, 2013; Chen *et al.*, 2015; Varga *et al.*, 2016; She *et al.*, 2021). As expected, the interlayer space of LDHs affected the catalytic activity. An *et al.* (2006) synthesized L-proline-intercalated MgAl LDH catalysts for an aldol reaction between benzaldehyde and acetone and reported that the decrease in the interlayer spacing (d_{003}) of LDHs decreased the catalytic activity. If the d_{003} value of HPW-intercalated LDHs could be tuned, the esterification activity of the LDHs could be controlled. In our most recent report (Wang *et al.*, 2020), a series of HPW-intercalated LDHs were synthesized and their d_{003} values were successfully tuned by varying the synthesis conditions. Moreover, increasing the d_{003} values improved the esterification activity for a model oil containing cyclohexanecarboxylic acid (CHCA).

However, the composition of NAs is complicated and varies with the source of crude oil (Wu *et al.*, 2019). In general, NAs composed of five- or six-membered rings and one carboxyl bonded to the rings or various side chains predominate in crude oil (Barrow *et al.*, 2009; Wu *et al.*, 2019). It is expected that the structure of NAs might affect the catalytic activity of HPW-intercalated LDHs. Moreover, the influence of the d_{003} value might vary among NAs with various structures. So far, there have been no reports investigating the effects of NA structure and the d_{003} values of HPW-intercalated LDHs on the esterification activity. During the present study, the effect of NA structure on the esterification activity over HPW-intercalated LDHs was investigated using NAs with various side chains and rings as reactants. Subsequently, the influence of the d_{003} value of HPW-intercalated LDHs on the esterification activity for NAs with various structures was studied using two LDHs with various d_{003} values as catalysts. In addition, the esterification kinetics of CHCA (a representative and widely used NA compound) over two such LDHs were investigated to further understand the role played by the interlayer spacing. Finally, the esterification reaction mechanism of CHCA was investigated based on product identification.

Experimental

Synthesis of LDHs

The HPW-intercalated MgAl LDHs were synthesized *via* an ion-exchange method using a nitrate MgAl LDH with an Mg/Al molar ratio of 2 as a precursor, which was prepared according to Wang *et al.* (2014a) and is referred to as Mg_2Al-NO_3. By tuning the exchange time, HPW-intercalated LDHs with various d_{003} values can be synthesized, as reported previously (Wang *et al.*, 2020). Herein, a HPW-intercalated LDH containing two LDH phases with d_{003} values of 1.46 and 1.07 nm was synthesized at 373 K for 1 h. This sample has the greatest ratio of the LDH phase with a d_{003} value of 1.46 nm to the LDH phase with a d_{003} value of 1.07 nm (Wang *et al.*, 2020). Another HPW-intercalated LDH containing only one LDH phase with a d_{003} value of 1.07 nm was synthesized at 373 K for 12 h. The two samples are referred to as Mg_2Al-PW-1 and Mg_2Al-PW-12, respectively. The brief synthesis procedure is as follows: firstly, 1 g of Mg_2Al-NO_3 was dispersed in deionized and CO_2-free water. Then, 2.78 g HPW was dissolved in 50 mL of water with pH adjusted to 4.5 using 1 M NaOH. The HPW solution was added dropwise to the above suspension and the pH of the mixture was adjusted to 4.5 using diluted HNO_3. Subsequently, the mixture was transferred into a three-necked flask equipped with a condenser and thermometer and maintained at 373 K for 1 or 12 h under vigorous stirring. Finally, the solid products were collected by filtration, washing and drying under vacuum at 353 K for 6 h.

Characterization of LDHs

X-ray diffraction (XRD) traces were recorded on an X'Pert Pro diffractometer (PANalytical, The Netherlands) using Cu-*K*α radiation, operated at 40 kV and 40 mA in the 2θ range of 5–70° with a scanning step of 0.02° and a counting time of 12 s per step.

Fourier-transform infrared (FTIR) spectra were recorded with a WQ520 spectrophotometer (Beifen, China) using the KBr pellet technique. A total of 32 scans with a resolution of 2 cm^{-1} were taken for each sample.

The composition (Mg, Al, P, W) of LDHs was measured *via* inductively coupled plasma atomic emission spectroscopy (ICP-AES) using an Optima 7300 V spectrometer (PerkinElmer, USA).

Esterification tests and kinetics

Six NAs with various structures including CHCA, cyclohexylacetic acid (CHAA), cyclohexylpropionic acid (CHPA), cyclohexylbutyric acid (CHBA), cyclopentanecarboxylic acid (CPCA) and benzoic acid (BA) were selected as model compounds to test the esterification activity of Mg_2Al-PW-1 and Mg_2Al-PW-12. The above NAs were diluted using a hydrotreated diesel to prepare a model oil with a TAN of 2 mg of KOH g^{-1}. For each esterification reaction, 20 g of model oil, 1 mL of EG and 0.2 g of LDHs were added to a three-necked flask equipped with a thermocouple, an electric motor stirrer and a condenser connected to a water separator. The mixture was heated in an oil bath at 423 K and maintained for 2 h under stirring. After the reaction, the liquid product was collected and its TAN was measured according to GB/T 258-2016. The deacidification ratio is calculated according to Equation 1, where TAN_0 and TAN_f refer to the TAN values of the oil before and after esterification, respectively.

$$\text{Deacidification ratio} = (TAN_0 - TAN_f)/TAN_0 \quad (1)$$

For the kinetics experiment, CHCA was dissolved in a hydrotreated diesel and the concentration was set at a TAN of 3 mg KOH g^{-1}, corresponding to a CHCA concentration of 0.06 mol L^{-1}. Then, 50 mL of oil, 2.5 mL of EG and 0.5 g of LDHs were added to the above apparatus. The reaction was performed at 373, 393, 413 and 433 K for 2 h. At each 20 min interval, 2 mL of

https://doi.org/10.1180/clm.2022.3 Published online by Cambridge University Press

liquid was taken out to measure the TAN. The concentration of CHCA (C_A) can be calculated using the TAN and the deacidification ratio.

For the reaction mechanism experiment, CHCA was dissolved in n-dodecane. After reaction at 423 K for 2 h, the liquid was separated from the suspension *via* filtration and analysed using gas chromatography and mass spectroscopy (GC-MS) on a 7890A gas chromatograph (Agilent, USA) coupled with a 5975C mass spectrometer (Agilent, USA) and equipped with an HP-5 MS capillary column (30 m × 250 μm × 0.25 μm). The temperature programme was as follows: from 323 to 443 K at a rate of 20 K min^{-1}, then 1 K min^{-1} up to 445 K, at which point it was maintained for 1 min, and finally 20 K min^{-1} up to 533 K. The GC injector and MS ion-source temperature were kept at 553 and 503 K, respectively. The MS detector was operated in the electron impact (EI) mode at 70 eV.

Results and discussion

Characterization of HPW-intercalated MgAl LDHs with various d_{003} *values*

As reported previously (Wang *et al.*, 2020), using a short exchange time, a mixed LDH with d_{003} values of 1.46 and 1.07 nm can be synthesized, whereas a prolonged exchange time induces the formation of a single LDH phase with a d_{003} value of 1.07 nm. Herein, the Mg_2Al-PW-1 contains two LDH phases with d_{003} values of 1.46 and 1.07 nm while Mg_2Al-PW-12 has a single LDH phase with a d_{003} value of 1.07 nm. These LDHs were chosen as esterification catalysts to investigate the effect of d_{003} values because the former has the greatest relative content of the LDH phase with a d_{003} value of 1.46 nm and the latter has the greatest relative content of the LDH phase with a d_{003} value of 1.07 nm. Their XRD traces and FTIR spectra are shown in Fig. 1a,b. Compared with the Mg_2Al-NO_3 precursor, the introduction of HPW leads to a shift in the (003) reflection from 9.9°2θ towards lower °2θ values, suggesting a larger interlayer spacing. The formation of two LDH phases with d_{003} values of 1.46 and 1.07 nm in Mg_2Al-PW-1 is attributed to the various orientations of HPW anions within the interlayer space: the 1.46 nm phase was mainly caused by $P_2W_{18}O_{62}^{6-}$ and $PW_{11}O_{39}^{7-}$ anions with their C2 axes tilted towards and perpendicular to the LDH layers, respectively, whereas the 1.07 nm phase was mainly produced *via* grafting of $PW_{12}O_{40}^{3-}$ anions onto the vacancies in the layers with their C2 axes perpendicular to the layers (Wang *et al.*, 2020). The relative content of the two LDHs phases determined by the ratio of the (003) peak area with a d_{003} value of 1.46 nm to that with a d_{003} value of 1.07 nm (Wang *et al.*, 2020) was 0.16 for Mg_2Al-PW-1. With a prolonged exchange time, the LDH phase with the d_{003} value of 1.07 nm dominated in the XRD trace of Mg_2Al-PW-12. For both LDHs, their FTIR spectra show the absence of a band at 1384 cm^{-1} assigned to the stretching vibration of nitrate and the presence of a series of bands at 1065, 965, 895 and 793 cm^{-1} assigned to the characteristic vibrations of HPW anions, confirming the complete replacement of nitrate by HPW anions. The HPW contents of Mg_2Al-PW-1 and Mg_2Al-PW-12 are 71.2% and 73.7%, respectively. The slightly greater HPW content of the latter LDH can be ascribed to its smaller Mg/Al ratio, which is due to the prolonged exchange time in the acidic system (Wang *et al.*, 2020).

Catalytic activity of NAs with various structures

To investigate the effects of the molecular structure of NAs on the catalytic esterification activities of HPW-intercalated LDHs with various d_{003} values, six NAs (CHCA, CHAA, CHPA, CHBA, CPCA and BA) that occur frequently in crude oil and petroleum fractions were chosen as model compounds because they can model more closely actual NA compositions in oils (Zhang *et al.*, 2006; Oh *et al.*, 2011). Their structures are shown in Scheme 1. Their molecular sizes obtained *via Material Studio* software using the *DMol*^{3} program (Gupta & Khatri, 2019) are listed in Table 1. The 3D models of the NAs are presented in Fig. S1. These NAs are classified by their chain length and rings. One class comprises CHCA, CHAA, CHPA and CHBA, which have the same six-membered ring but various side chains. The other class includes CPCA, BA and CHCA, which have the same side chain but various rings. Note that BA is not strictly a NA, but the six compounds will be categorized collectively as NAs for convenience (Wu *et al.*, 2017a). The esterification activities of the two classes of NAs over Mg_2Al-PW-12 are discussed. Following this, the esterification activities of these NAs over two LDHs with various d_{003} values (Mg_2Al-PW-12 and Mg_2Al-PW-1) are compared.

The deacidification ratios of the NAs with various side chains over Mg_2Al-PW-12 are listed in Table 1. The catalytic activities follow the order CHAA > CHPA > CHBA > CHCA, which follows directly the molecule size of the NAs, except for CHCA. Although CHCA has the smallest size, it is a secondary carboxyl acid and thus displays greater steric hindrance in esterification than the other three primary carboxyl acids (Takahashi *et al.*, 1989). The NAs and alcohol reactants might enter the interlayer space of LDHs to interact with the acidic catalytic sites induced by HPW and thus generate the ester products that diffuse into the bulk solution (Wu *et al.*, 2017b). This might be considered to be an interlayer catalytic esterification reaction. The NAs with smaller molecule sizes prefer to enter the interlayer of LDHs, leading to improved deacidification ratios. Silva *et al.* (2013) used clays as adsorbents for removing NAs from a model crude oil and also reported that the mass transfer coefficients of CPCA, CHAA and CHBA in the adsorbent decreased with increasing molecule size. In addition to the molecular size, the reactivity of these NAs is also related to the inductive effect. For esterification catalysed by acidic sites, the nucleophilic species generated from the deprotonation of the alcohol –OH can attack the carbocation of the carboxylic acid formed *via* the interaction between the acidic sites in catalysts and carbonyl oxygen, generating an intermediate that finally eliminates water to produce ester (Zeng *et al.*, 2012). As the chain length of the carboxylic acid increases, the inductive effect increases the electron-donating ability of carboxylic acid and favours the protonation of the carboxylate oxygen. However, this leads to lower electrophilicity of the carbonyl carbon and thus the rate-limiting nucleophilic attack by alcohol is hindered significantly, thus reducing the esterification activity of carboxylic acids with longer chains (Srilatha *et al.*, 2009; Osatiashtiani *et al.*, 2016).

The deacidification ratios of CPCA, CHCA and BA, which have the same side chain but various rings, over Mg_2Al-PW-12 are also listed in Table 1. The activities follow the order CPCA > CHCA > BA. Among the three NAs, CPCA has the smallest molecule size and so is more able to enter the interlayer. Moreover, the steric substituent constant of cyclo-C_5H_9 is smaller than that for cyclo-C_6H_{11} (Hirota *et al.*, 2001; Osatiashtiani *et al.*,

https://doi.org/10.1180/clm.2022.3 Published online by Cambridge University Press

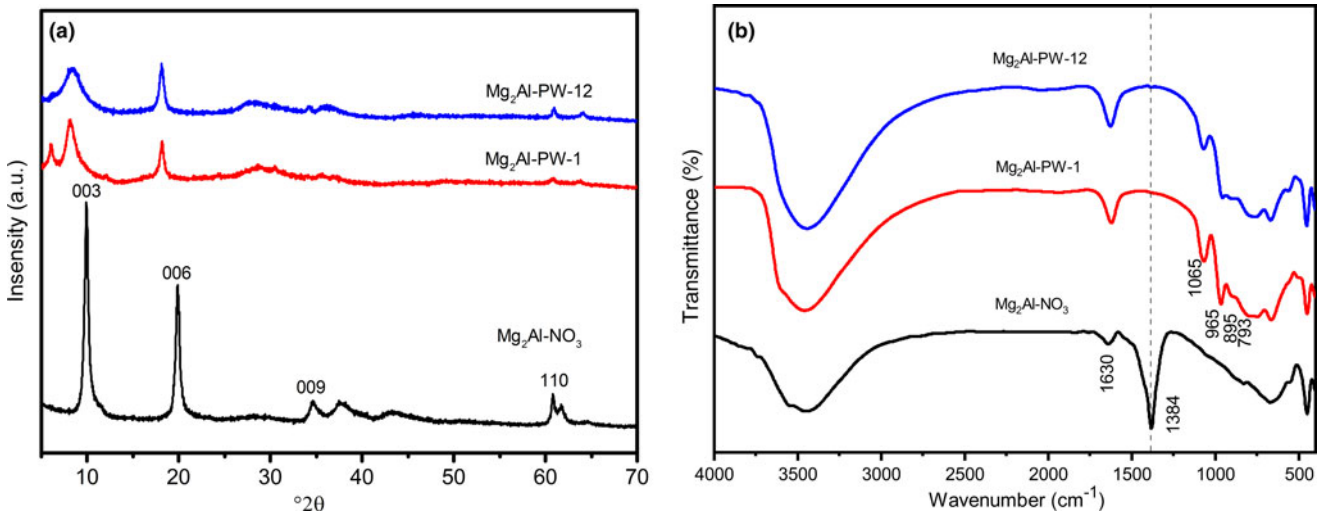

Fig. 1. (a) XRD traces and (b) FTIR spectra of the nitrate LDH precursor and HPW-intercalated LDHs with various d_{003} values.

Molecule structure	Chemical name	Abbreviation	Molecule structure	Chemical name	Abbreviation
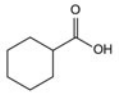	cyclohexanecarboxylic acid	CHCA	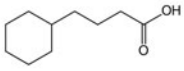	cyclohexylbutyric acid	CHBA
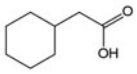	cyclohexylacetic acid	CHAA	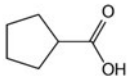	cyclopentanecarboxylic acid	CPCA
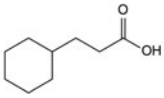	cyclohexylpropionic acid	CHPA	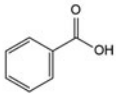	benzoic acid	BA

Scheme 1. Molecule structures of the NA model compounds.

Table 1. Deacidification ratios for NAs with various structures over two LDHs.

NAs	Deacidification ratio (%)		Increment in deacidification ratio (%)[a]	Molecule size of NAs (nm)
	Mg_2Al-PW-1	Mg_2Al-PW-12		
CHCA	85.9	74.2	15.8	0.70
CHAA	92.5	80.5	14.9	0.76
CHPA	90.6	78.1	16.1	0.87
CHBA	89.5	76.1	17.6	1.00
CPCA	86.5	75.1	15.2	0.64
BA	82.1	73.3	11.9	0.69

[a] The increment in deacidification ratio is calculated from the deacidification ratio difference between Mg_2Al-PW-1 and Mg_2Al-PW-12 divided by the deacidification ratio of Mg_2Al-PW-12.

2016). Steric hindrance of carboxylic acids might induce electronic repulsion between the non-bonded atoms of reacting molecules, which might reduce the electron density in the intermolecular region and hinder bonding interactions, leading to poor reactivity for acid-catalysed esterification (Liu *et al.*, 2006). Although the molecule size of BA is slightly smaller than that of CHCA (0.69 *vs* 0.70 nm), its carboxyl group is directly bonded with an aromatic ring, leading to conjugation between them. In general, conjugated carboxyl groups are less reactive than non-conjugated ones in esterification reactions (Anand *et al.*, 1999) because the electron-donating effect of the aromatic ring might reduce the electrophilicity of carbon in the carbonyl (Sun *et al.*, 2006). As a result, esterification of BA is more difficult to achieve than that of CHCA, which is in accordance with previous work (Takahashi *et al.*, 1989; Ram & Chalres, 1997).

Mg_2Al-PW-1 was also used as an esterification catalyst for NAs, and the results of this process are listed in Table 1. The order of deacidification ratios for the NAs follows a similar trend to that over Mg_2Al-PW-12. For each NA, the deacidification ratio over Mg_2Al-PW-1 is much greater than that over Mg_2Al-PW-12. This can be attributed to the larger d_{003} value of Mg_2Al-PW-1, which facilitates reactant diffusion into the larger interlayer space. To compare the degree of improvement of the deacidification ratios caused by the greater d_{003} value, the increments in the deacidification ratios over the two LDHs for each NA are listed in Table 1. The enlarged interlayer space improves activity more significantly for the NAs with larger molecule sizes than for those with smaller molecule sizes. For CHBA, which has the greatest molecule size, the deacidification ratio over Mg_2Al-PW-1 was increased by 17.6% when compared to that

https://doi.org/10.1180/clm.2022.3 Published online by Cambridge University Press

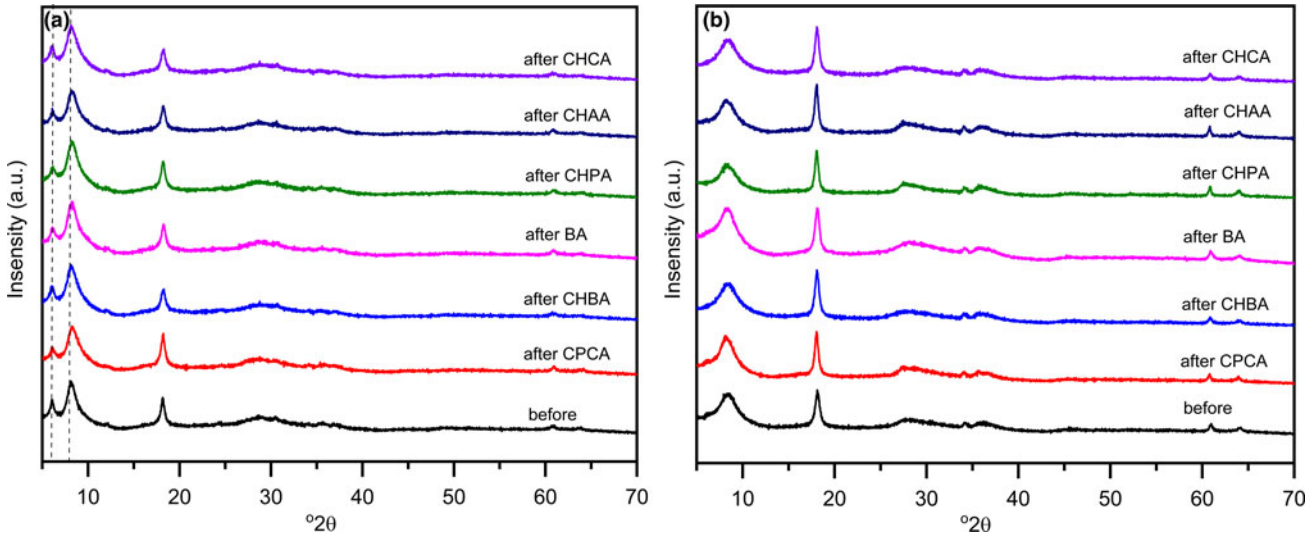

Fig. 2. XRD traces of (a) Mg_2Al-PW-1 and (b) Mg_2Al-PW-12 after reaction with NAs of various structures.

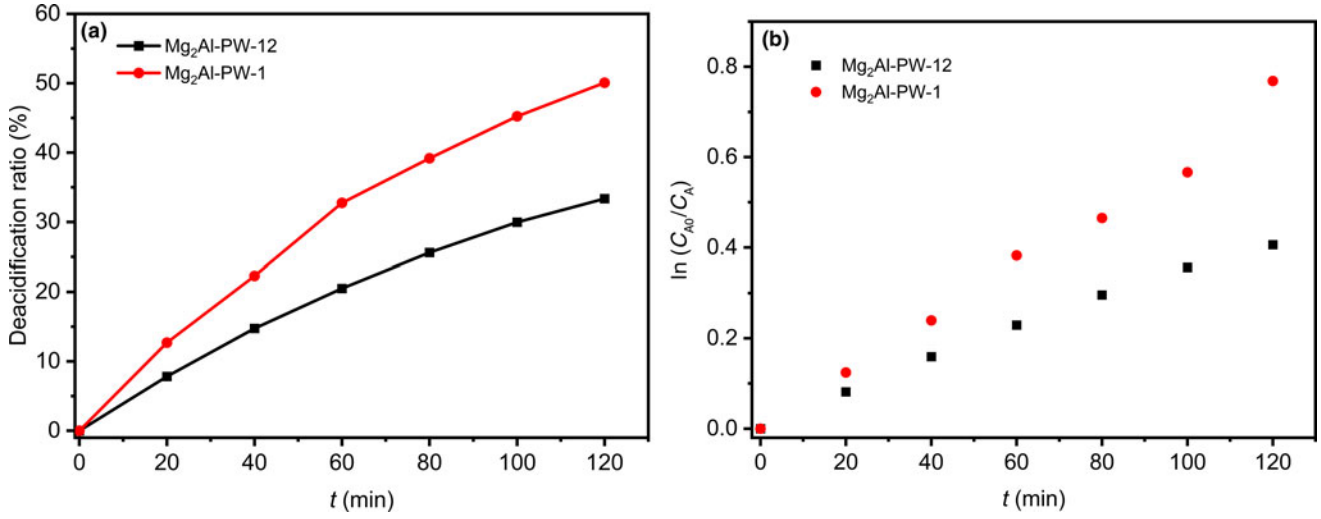

Fig. 3. Plots of (a) deacidification ratio and (b) CHCA concentration as a function of reaction time over catalysts Mg_2Al-PW-1 and Mg_2Al-PW-12 at 373 K.

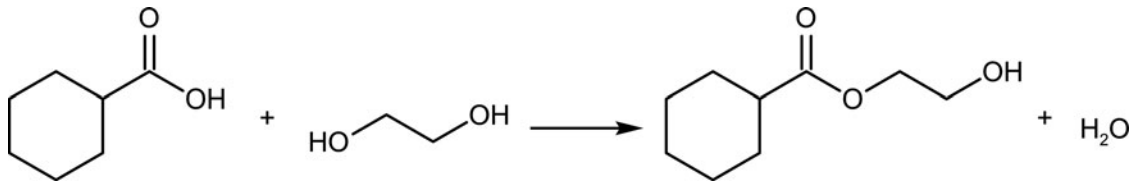

Scheme 2. Esterification between CHCA and EG.

over Mg_2Al-PW-12, which is the greatest increment among the NAs. Varga *et al.* (2016) synthesized two Mn(II)-L-cysteine complex-intercalated CaAl LDHs with d_{003} values of 0.86 and 0.92 nm as catalysts for the epoxidation of cyclohexene. The conversion of cyclohexene over the latter LDH was greater than that over the former due to the increased d_{003} value, which reduced diffusion resistance. For CHCA with its steric hindrance, the catalyst with a greater d_{003} value increased the deacidification ratio by 15.8%, which indicates that a greater d_{003} value also aids NAs with steric hindrance to access the catalytic sites in LDHs. Among all of the NAs, the deacidification ratio increment of BA is the smallest. This might suggest that the interlayer spacing has a relatively limited influence on reactions controlled by the electronic effect. Mg_2Al-PW-1 has fewer total acidic sites and a smaller specific surface area than Mg_2Al-PW-12; therefore, the enhancement in the esterification activity for NAs with various structures over Mg_2Al-PW-1 might be attributed mainly to the larger interlayer spacing (Wang *et al.*, 2020).

https://doi.org/10.1180/clm.2022.3 Published online by Cambridge University Press

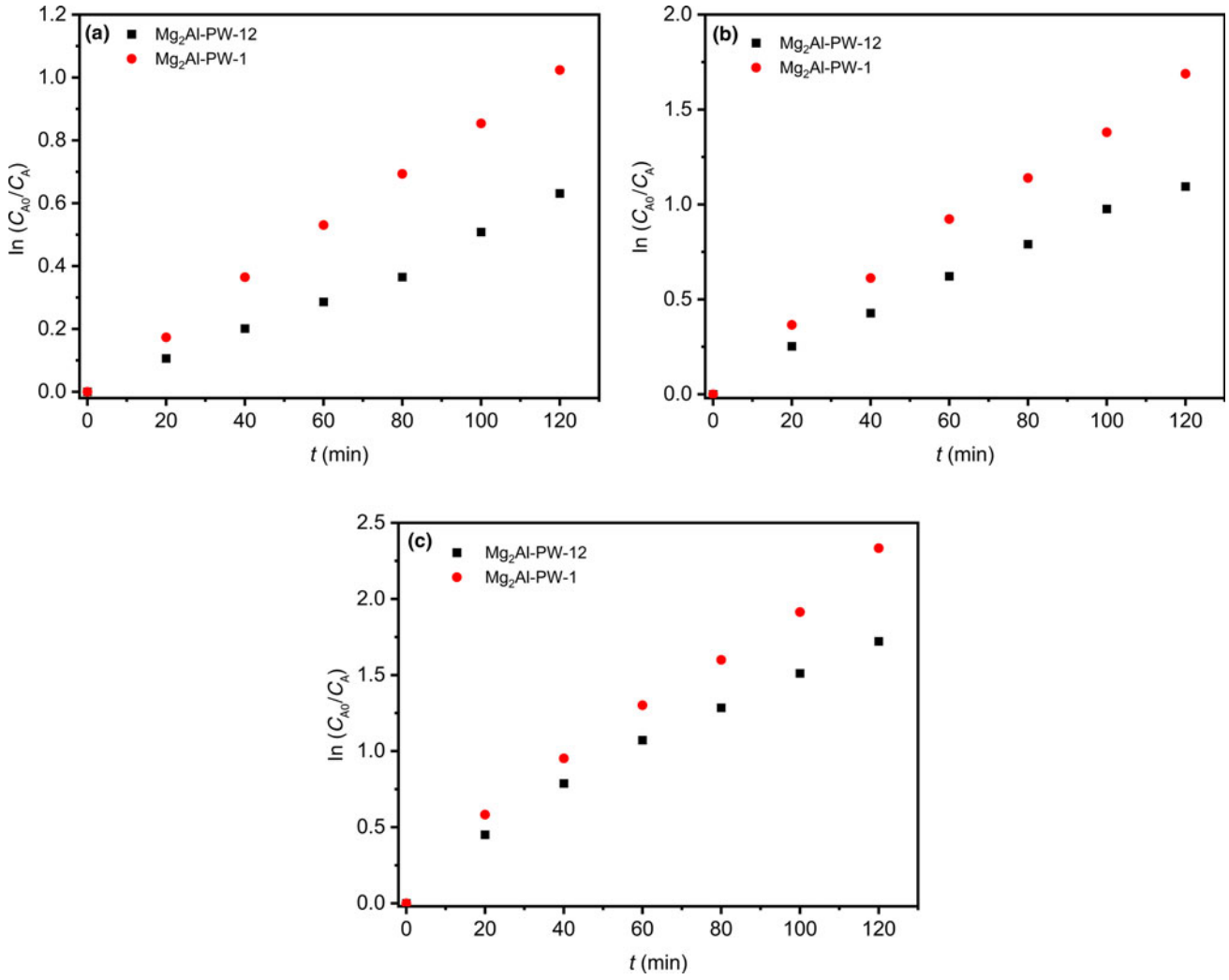

Fig. 4. Plots of CHCA concentration as a function of reaction time over catalysts Mg_2Al-PW-1 and Mg_2Al-PW-12 at (a) 393 K, (b) 413 K and (c) 433 K.

Table 2. The correlation coefficients (R^2) and rate constants (k) for esterification at various temperatures.

	Mg_2Al-PW-12		Mg_2Al-PW-1	
Temperature (K)	k (10^{-3} min^{-1})	R^2	k (10^{-3} min^{-1})	R^2
373	3.41	0.994	6.15	0.981
393	5.12	0.992	8.51	0.996
413	9.08	0.993	13.50	0.992
433	13.90	0.978	18.40	0.989

All catalysts after reactions with the NAs of various structures were recovered *via* filtration and washing with toluene. Their XRD traces are shown in Fig. 2. No obvious changes in reflections are observed in the two series of catalysts before and after the reaction; therefore, the structures of the LDHs were retained.

Reaction kinetics

The esterification kinetics over Mg_2Al-PW-1 and Mg_2Al-PW-12 were studied using CHCA as a model compound because CHCA represents closely the NAs in petroleum fractions due to its representative structural features (Zhang *et al.*, 2006, 2016; Manan *et al.*, 2012) and because it is less reactive than other NAs, as shown in Table 1. Kinetics studies of the model compound (which is difficult to handle) would offer useful information for understanding the catalyst's behaviour and for designing the actual industrial process (Krishnamoorthy *et al.*, 1998; Kaisalo *et al.*, 2016). To eliminate the limitation of mass transfer, a series of preliminary experiments was performed. Catalysts with various particle sizes (i.e. 40–60, 20–40 and 10–20 mesh) were tested. The stirring speed during the reaction was adjusted. The deacidification ratio is nearly constant at sizes <10–20 mesh and for stirring speeds >200 rpm. This demonstrates that the mass transfer limitation can be removed with a catalyst particle size of 20–40 mesh and a stirring speed of 300 rpm. Therefore, the kinetics experiments were carried out under such conditions.

The variation of deacidification ratio with reaction time over Mg_2Al-PW-1 and Mg_2Al-PW-12 at a temperature of 373 K is shown in Fig. 3a. The esterification between CHCA and EG can be expressed as in Scheme 2. Due to the excessive EG and the continuous removal of water from the reaction, the esterification rate (r_A) can be described as in Equation 2, in which n is the reaction order (Huang *et al.*, 2011). Due to the great excess of EG, this

https://doi.org/10.1180/clm.2022.3 Published online by Cambridge University Press

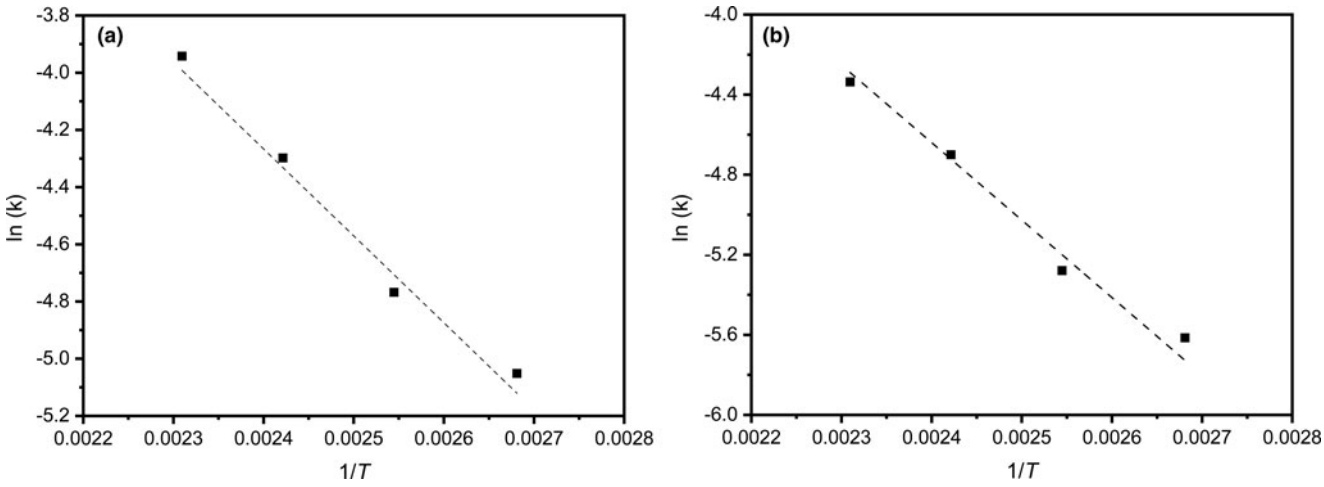

Fig. 5. Arrhenius plots (ln(k) *vs* 1/*T*) of (a) Mg_2Al-PW-1 and (b) Mg_2Al-PW-12.

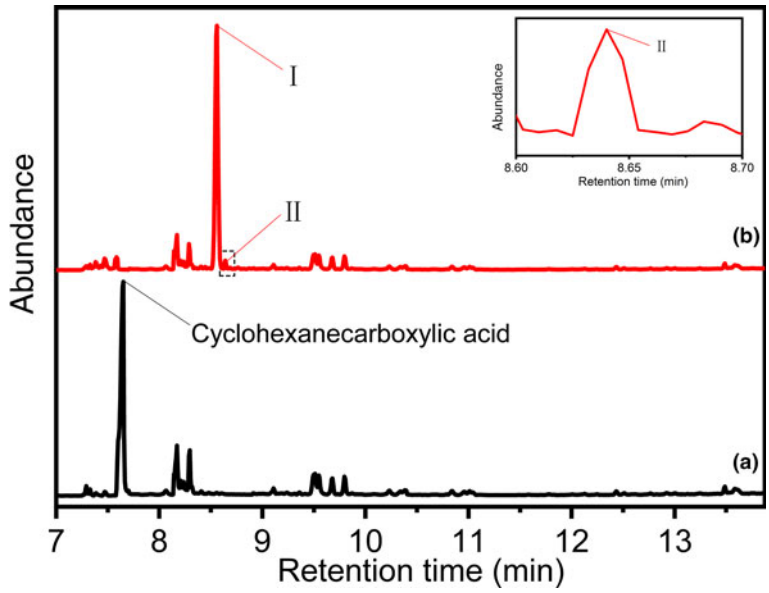

Fig. 6. Total ion chromatograms of (a) feed and (b) products over Mg_2Al-PW-1 catalyst. I and II refer to ester product I and ester product II, respectively.

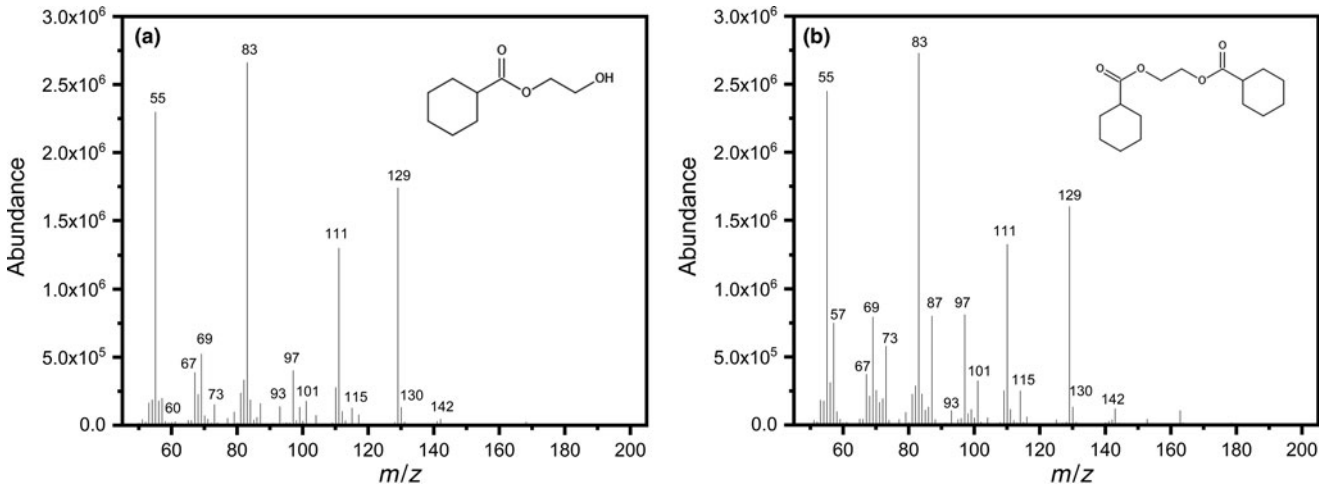

Fig. 7. Mass spectra of (a) ester product I and (b) ester product II.

https://doi.org/10.1180/clm.2022.3 Published online by Cambridge University Press

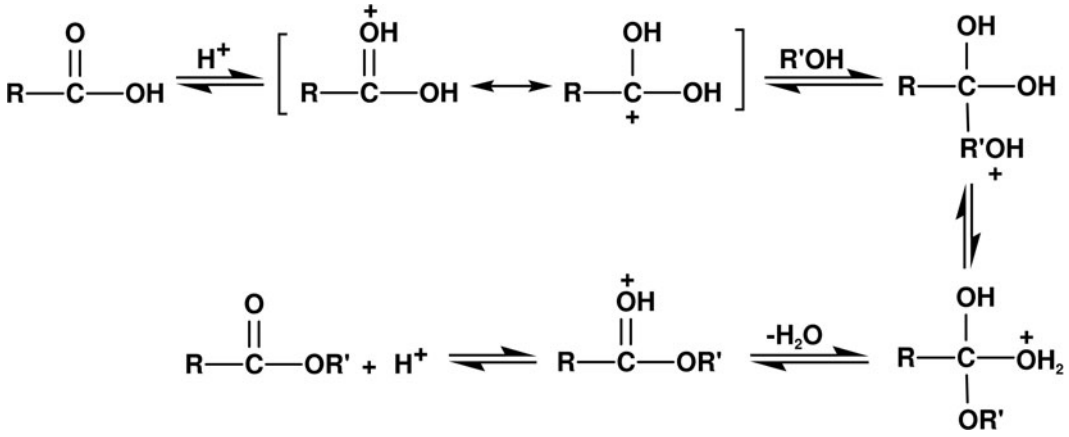

Scheme 3. Possible esterification mechanism of NA and alcohol.

reaction might be safely assumed to be first order (Zeng *et al.*, 2012; Patel & Brahmkhatri, 2013). By integrating the reaction time from 0 to t, the kinetics equation can be converted to Equation 3, where C_{A0} is the initial concentration of CHCA. The plot of $\ln(C_{A0}/C_A)$ *vs* time (t) is shown in Fig. 3b, demonstrating a linear relationship between CHCA consumption and reaction time. The rate constant (k) can be obtained from the slope of the linear equation. Such kinetics experiments were also performed at 393, 413 and 433 K. The plots of $\ln(C_{A0}/C_A)$ *vs t* are shown in Fig. 4. All of the plots show linear relationships for both catalysts. Table 2 lists the values of the coefficient of determination (R^2) and k for the esterification reactions over the two catalysts at each reaction temperature. The high R^2 values demonstrate the adequacy of the first-order reaction model (Al-Saadi *et al.*, 2020), which is in accordance with Cardoso *et al.* (2008). With increasing temperature, the value of k increased. All k values over Mg_2Al-PW-1 are greater than those over Mg_2Al-PW-12, regardless of the reaction temperature.

$$r_A = -\frac{dC_A}{dt} = kC_A^n \quad (2)$$

$$\ln\frac{C_{A0}}{C_A} = kt \quad (3)$$

The Arrhenius equation was applied to calculate the activation energy (E_a) over the two catalysts. The plot of ln(k) *vs* $1/T$ is shown in Fig. 5 and the value of E_a was determined from the slope of plot. The E_a values are 26.25 kJ mol^{-1} for Mg_2Al-PW-1 and 32.18 kJ mol^{-1} for Mg_2Al-PW-12. These values lie within the range of E_a reported in previous works on the esterification of NAs over ZnAl LDH and MgAl LDH catalysts (Huang *et al.*, 2011; Li *et al.*, 2013; Redondo *et al.*, 2020). The smaller E_a of Mg_2Al-PW-1 compared to that of Mg_2Al-PW-12 further demonstrates that the enlarged interlayer space accelerates the reaction in the interlayer.

Mechanism of esterification

To investigate the mechanism of esterification between CHCA and EG, the reaction was performed in an n-dodecane solvent over the Mg_2Al-PW-1 catalyst. The feed and products were detected using GC-MS and their total ion chromatograms are shown in Fig. 6. For the feed, the strong peak at the retention time of 7.64 min is attributed to CHCA. After the reaction, this peak nearly disappears, while a strong peak (I in Fig. 6) at 8.56 min and a very weak peak (II in Fig. 6) at 8.64 min are observed. The mass spectra of I and II are shown in Fig. 7. Following identification in the National Institute of Standards and Technology (NIST) database, I and II can be assigned to 2-hydroxyethyl cyclohexanecarboxylate (CAS 16179-44-5) and 2-(cyclohexanecarbonyloxy) ethyl cyclohexanecarboxylate (CAS 22735-96-2), respectively. The GC-MS results suggest that the reaction between CHCA and EG tends to form unilateral ester I rather than bilateral ester II.

Previous research revealed that HPW-intercalated LDHs would offer greater numbers of stronger acidic sites than their nitrate precursor (Wu *et al.*, 2017b). This increased acidity is responsible for the esterification activity. A blank esterification experiment for CHCA over the Mg_2Al-NO_3 precursor was performed and the deacidification ratio obtained was 33.9% (i.e. much lower than that over HPW-intercalated LDHs). Based on the acid-catalysed esterification theory (Rana *et al.*, 2018), the GC-MS results and the origin of the acid sites in HPW-intercalated LDHs (Wu *et al.*, 2017b), the reaction mechanism of esterification over Mg_2Al-PW-1 could be proposed as follows (Scheme 3): firstly, the acidic sites in the catalyst can interact with the oxygen atoms in the carbonyls of the NA, leading to the increased electrophilicity of the carbon atoms in the carbonyls; secondly, such species may be attacked by the nucleophile hydroxyl in the alcohol to form intermediates. Undergoing a series of rearrangement and dehydration reactions, such intermediates can finally be converted to ester, and then the catalyst is recovered (Li *et al.*, 2007).

Conclusion

Two HPW-intercalated MgAl LDHs with various interlayer spacings (d_{003} values of 1.46 and 1.07 nm) were used as catalysts for the esterification of NAs with various structures. For CHCA, CHAA, CHPA and CHBA, which have the same ring but various side chains, the esterification activity decreased with increasing chain length, except for CHCA, because CHCA is a secondary carboxyl acid. For CHCA, CPCA and BA, which have the same side chain but various rings, the esterification activity decreased with increasing molecular size, except for BA, because BA has a

https://doi.org/10.1180/clm.2022.3 Published online by Cambridge University Press

conjugated carboxyl group. The LDH with a greater d_{003} value can improve significantly the activity for all NAs, being particularly effective for the NAs with greater molecule sizes and steric hindrances. The esterification reactions over both LDHs follow first-order kinetics, while the LDH with a greater d_{003} value can reduce the E_a by 18.4%. Due to the catalytic sites being in the interlayer, reactants must move to the edge of the interlayer or enter the interlayer to come into contact with the catalytic sites. Therefore, an enlarged interlayer spacing would facilitate the reactants diffusing into the interlayer and thus improve catalytic activity. Product identification shows that unilateral ester is the dominant product. The present investigation reveals the influences of NA structures and the interlayer spacing on the esterification activity of HPW-intercalated LDHs. It may offer an alternative for enhancing the esterification activity of HPW-intercalated LDHs for removing NAs from petroleum by enlarging the interlayer spacing.

Supplementary material. To view supplementary material for this article, please visit https://doi.org/10.1180/clm.2022.3.

Financial support. The authors acknowledge financial support from the National Natural Science Foundation of China (Project No. 21978242).

References

Al-Saadi A., Mathan B. & He Y. (2020) Esterification and transesterification over SrO–ZnO/Al_2O_3 as a novel bifunctional catalyst for biodiesel production. *Renewable Energy*, **158**, 388–399.

An Z., Zhang W., Shi H. & He J. (2006) An effective heterogeneous l-proline catalyst for the asymmetric aldol reaction using anionic clays as intercalated support. *Journal of Catalysis*, **241**, 319–327.

Anand R.C., Milhotra V. & Milhotra A. (1999) Selective esterification of nonconjugated carboxylic acids in the presence of conjugated or aromatic carboxylic acids under mild conditions. *Journal of Chemical Research*, **23**, 378–379.

Barrow M.P., Headley J.V., Peru K.M. & Derrick P.J. (2009) Data visualization for the characterization of naphthenic acids within petroleum samples. *Energy Fuels*, **23**, 2592–2599.

Cardoso A.L., Augusti R. & Silva M.J.D. (2008) Investigation on the esterification of fatty acids catalyzed by the $H_3PW_{12}O_{40}$ heteropolyacid. *Journal of the American Oil Chemists' Society*, **85**, 555–560.

Chen Y., Yao Z., Miras H.N. & Song Y.-F. (2015) Modular polyoxometalate-layered double hydroxide composites as efficient oxidative catalysts. *Chemistry: A European Journal*, **21**, 10812–10820.

Das J. & Parida K.M. (2007) Heteropoly acid intercalated Zn/Al HTlc as efficient catalyst for esterification of acetic acid using n-butanol. *Journal of Molecular Catalysis A: Chemical*, **264**, 248–254.

Enferadi-Kerenkan A., Do T.-O. & Kaliaguine S. (2018) Heterogeneous catalysis by tungsten-based heteropoly compounds. *Catalysis Science Technology*, **8**, 2257–2284.

Guo Y., Li D., Hu C., Wang Y. & Wang E. (2001) Layered double hydroxides pillared by tungsten polyoxometalates: synthesis and photocatalytic activity. *International Journal of Inorganic Materials*, **3**, 347–355.

Gupta K. & Khatri O.P. (2019) Fast and efficient adsorptive removal of organic dyes and active pharmaceutical ingredient by microporous carbon: effect of molecular size and charge. *Chemical Engineering Journal*, **378**, 122218.

Hirota M., Sakakibara K., Yuzuri T. & Kuroda S. (2001) Evaluation of the steric substituent effect by ΩS: reinvestigation of the reaction dependency of the steric substituent constant. *Journal of Physical Organic Chemistry*, **14**, 788–793.

Hu C., Zhang X., Xu L., Mu B., Zu W. & Wang E. (1998) Oxidative catalysis of Keggin anion $[XW_{11}O_{39}Z(H_2O)]^{n-}$ pillared clays in the reaction of acetaldehyde with H_2O_2. *Applied Clay Science*, **13**, 495–511.

Huang Y., Zhu J., Wu B., Wang Y. & Fang L. (2011) Esterification kinetics of cyclohexanecarboxylic acid and ethylene glycol in diesel oil with or without a ZnAl-HTlc catalyst. *Petroleum Science and Technology*, **29**, 2209–2219.

Kaisalo N., Simell P. & Lehtonen J. (2016) Benzene steam reforming kinetics in biomass gasification gas cleaning. *Fuel*, **182**, 696–703.

Khan M.K., Riaz A., Yi M. & Kim J. (2017) Removal of naphthenic acids from high acid crude *via* esterification with methanol. *Fuel Processing Technology*, **165**, 123–130.

Krishnamoorthy S., Baker J.P. & Amiridis M.D. (1998) Catalytic oxidation of 1,2-dichlorobenzene over V_2O_5/TiO_2-based catalysts. *Catalysis Today*, **40**, 39–46.

Li G., Li X. & Eli W. (2007) Solvent-free esterification catalyzed by surfactant-combined catalysts at room temperature. *New Journal of Chemistry*, **31**, 348–351.

Li X., Zhu J., Liu Q. & Wu B. (2013) The removal of naphthenic acids from dewaxed VGO *via* esterification catalyzed by Mg–Al hydrotalcite. *Fuel Processing Technology*, **111**, 68–77.

Liu Y., Lotero E. & Goodwin J.G. (2006) Effect of carbon chain length on esterification of carboxylic acids with methanol using acid catalysis. *Journal of Catalysis*, **243**, 221–228.

Liu Y., An Z., Zhao L., Liu H. & He J. (2013) Enhanced catalytic efficiency in the epoxidation of alkenes for manganese complex encapsulated in the hydrophobic interlayer region of layered double hydroxides. *Industrial & Engineering Chemistry Research*, **52**, 17821–17828.

Lopez-Salinas E., Hernandez-Cortez J., Schifter I., Torres-Garcıa E., Navarrete J., Gutierrez-Carrillo A. *et al.* (2000) Thermal stability of 12-tungstophosphoric acid supported on zirconia. *Applied Catalysis A: General*, **193**, 215–225.

Manan N.A., Atkins M.P., Jacquemin J., Hardacre C. & Rooney D.W. (2012) Phase equilibria of binary and ternary systems containing ILs, dodecane, and cyclohexanecarboxylic acid. *Separation Science and Technology*, **47**, 312–324.

Mao N., Zhou C., Tong D., Yu W. & Lin C.X.C. (2017) Exfoliation of layered double hydroxide solids into functional nanosheets. *Applied Clay Science*, **144**, 60–78.

Ma J., Yang M., Chen Q., Zhang S., Cheng H., Wang S. *et al.* (2017) Comparative study of Keggin-type polyoxometalate pillared layered double hydroxides *via* two synthetic routes: characterization and catalytic behavior in green epoxidation of cyclohexene. *Applied Clay Science*, **150**, 210–216.

Oh H.Y., Park J.H., Rhee Y.W. & Kim J.N. (2011) Decarboxylation of naphthenic acid using alkaline earth metal oxide. *Journal of Industrial and Engineering Chemistry*, **17**, 788–793.

Omwoma S., Chen W., Tsunashima R. & Song Y.-F. (2014) Recent advances on polyoxometalates intercalated layered double hydroxides: from synthetic approaches to functional material applications. *Coordination Chemistry Reviews*, **258–259**, 58–71.

Osatiashtiani A., Durndell L.J., Manayil J.C., Lee A.F. & Wilson K. (2016) Influence of alkyl chain length on sulfated zirconia catalysed batch and continuous esterification of carboxylic acids by light alcohols. *Green Chemistry*, **18**, 5529–5535.

Patel A. & Brahmkhatri V. (2013) Kinetic study of oleic acid esterification over 12-tungstophosphoric acid catalyst anchored to different mesoporous silica supports. *Fuel Processing Technology*, **113**, 141–149.

Ram R.N. & Charles I. (1997) Selective esterification of aliphatic nonconjugated carboxylic acids in the presence of aromatic or conjugated carboxylic acids catalysed by $NiCl_2.6H_2O$. *Tetrahedron*, **53**, 7335–7340.

Rana B.S., Cho D.-W., Cho K. & Kim J.-N. (2018) Total acid number (TAN) reduction of high acidic crude oil by catalytic esterification of naphthenic acids in fixed-bed continuous flow reactor. *Fuel*, **231**, 271–280.

Redondo N., Dieuzeide M.L. & Amadeo N. (2020) Acid removal from crude oils by catalytic esterification naphthenic acid catalize by Mg/Al hydrotalcite. *Catalysis Today*, **353**, 82–87.

She Q., Liu J., Aymonier C. & Zhou C. (2021) *In situ* fabrication of layered double hydroxide film immobilizing gold nanoparticles in capillary microreactor for efficient catalytic carbonylation of glycerol. *Molecular Catalysis*, **513**, 111825.

Shi H. & He J. (2011) Orientated intercalation of tartrate as chiral ligand to impact asymmetric catalysis. *Journal of Catalysis*, **279**, 155–162.

Shi H., Yu C. & He J. (2010) Constraining titanium tartrate in the interlayer space of layered double hydroxides induces enantioselectivity. *Journal of Catalysis*, **271**, 79–87.

Silva J.P., Costa A.L., Chiaro S.S., Delgado B.E., De Figueiredo M.A. & Senna L.F. (2013) Carboxylic acid removal from model petroleum

fractions by a commercial clay adsorbent. *Fuel Processing Technology*, **112**, 57–63.

Srilatha K., Lingaiah N., Sai-Prasad P.S., Prabhavathi-Devi B.L.A., Prasad R.B.N. & Venkateswar S. (2009) Influence of carbon chain length and unsaturation on the esterification activity of fatty acids on Nb_2O_5 catalyst. *Industrial Engineering Chemistry Research*, **48**, 10816–10819.

Sun H., Hua R. & Yin Y. (2006) $ZrOCl_2{\cdot}8H_2O$: an efficient, cheap and reusable catalyst for the esterification of acrylic acid and other carboxylic acids with equimolar amounts of alcohols. *Molecules*, **11**, 263–271.

Takahashi K., Shibagaki M. & Matsushita H. (1989) The esterification of carboxylic acid with alcohol over hydrous zirconium oxide. *Bulletin of the Chemical Society of Japan*, **62**, 2353–2361.

Varga G., Kukovecz Á., Kónya Z., Korecz L., Muráth S., Csendes Z. *et al.* (2016) Mn(II)-amino acid complexes intercalated in CaAl-layered double hydroxide – well-characterized, highly efficient, recyclable oxidation catalysts. *Journal of Catalysis*, **335**, 125–134.

Wang H., Duan W., Wu Y., Tang Y. & Li L. (2014a) Synthesis of magnesium–aluminum layered double hydroxide intercalated with ethylene glycol by the aid of alkoxides. *Inorganica Chimica Acta*, **418**, 163–170.

Wang Y., Li J., Sun X., Duan H., Song C., Zhang M. & Liu Y. (2014b) Removal of naphthenic acids from crude oils by fixed-bed catalytic esterification. *Fuel*, **116**, 723–728.

Wang H., Duan W., Lei Y., Wu Y., Guo K. & Wang X. (2015) An intracrystalline catalytic esterification reaction between ethylene glycol intercalated layered double hydroxide and cyclohexanecarboxylic acid. *Catalysis Communications*, **62**, 44–47.

Wang H., Yang Z., Zhan X., Wu Y. & Li M. (2017) NiAlZrW hydrodesulfurization catalysts derived from tungstate intercalated NiAlZr layered double hydroxides. *Fuel Processing Technology*, **160**, 178–184.

Wang H., Li D., Wu Y. & Ding Y. (2020) Preparation of tungstophosphoric acid intercalated MgAl layered double hydroxides with a tunable interlayer spacing and their catalytic esterification performance in the deacidification of model crude oil. *Journal of Fuel Chemistry and Technology*, **48**, 44–51.

Wu C., Visscher A.D. & Gates I.D. (2017a) Molecular interactions between 1-butyl-3-methylimidazolium tetrafluoroborate and model naphthenic acids: a DFT study. *Journal of Molecular Liquids*, **243**, 462–471.

Wu Y., Liu X., Lei Y., Qiu Y., Wang M. & Wang H. (2017b) Synthesis and characterization of 12-tungstophosphoric acid intercalated layered double hydroxides and their application as esterification catalysts for deacidification of crude oil. *Applied Clay Science*, **150**, 34–41.

Wu C., Visscher A.D. & Gates I.D. (2019) On naphthenic acids removal from crude oil and oil sands process-affected water. *Fuel*, **253**, 1229–1246.

Zeng Z., Li C., Xue W., Chen J. & Che Y. (2012) Recent developments on the mechanism and kinetics of esterification reaction promoted by various catalysts. Pp. 255–282 in: *Chemical Kinetics* (V. Patel, editor). IntechOpen, London UK.

Zhang A., Ma Q., Wang K., Liu X., Shuler P. & Tang Y. (2006) Naphthenic acid removal from crude oil through catalytic decarboxylation on magnesium oxide. *Applied Catalysis A: General*, **303**, 103–109.

Zhang Y., Klamerth N. & El-Din M.G. (2016) Degradation of a model naphthenic acid by nitrilotriacetic acid – modified Fenton process. *Chemical Engineering Journal*, **292**, 340–347.

https://doi.org/10.1180/clm.2022.3 Published online by Cambridge University Press